Macromolecules

Article

pubs.acs.org/Macromolecules

ESA-CF Synthesis of Linear and Cyclic Polymers Having Densely Appended Perylene Units and Topology Effects on Their Thin-Film Electron Mobility

Akihiro Kimura, Tsukasa Hasegawa, Takuya Yamamoto, Hidetoshi Matsumoto, and Yasuyuki Tezuka*

Department of Organic and Polymeric Materials, Tokyo Institute of Technology, O-okayama, Meguro-ku, Tokyo 152-8552, Japan

Supporting Information

ABSTRACT: A pair of topologically contrastive, linear and cyclic polymers having densely appended perylene diimide (PDI) units have been prepared by means of an electrostatic self-assembly and covalent fixation (ESA-CF) process, using an assembly composed of either linear or cyclic polyacrylate anions of different segment lengths (DP_n = 50, 93, and 128) accompanying countercations of a perylene diimide (PDI) derivative having a cyclic ammonium salt group (**II_L**/**III** and **II_C**/**III**, respectively). The subsequent heating treatment at 180 °C produced the covalently converted product, i.e., the linear **IV_L** and the cyclic **IV_C**, respectively, in which the PDI unit was introduced nearly quantitatively to the backbone acrylate units. The obtained linear and cyclic polymers having pendant PDI units were observed to form commonly spherical self-assemblies both in bulk and in solution states, while the solution viscosity was noticeably higher with the linear products than with the cyclic counterparts. The electron-only device (EOD) measurement by using thin-film samples of a series of cyclized products, **IV_C**, revealed consistently higher electron carrier mobilities in comparison with the corresponding linear counterparts, **IV_L**.

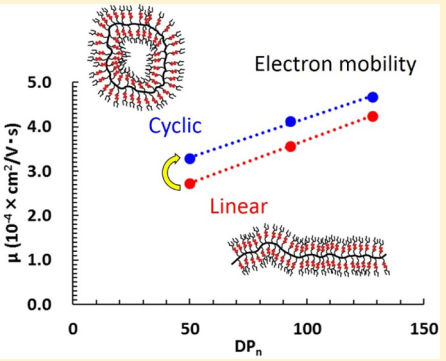

INTRODUCTION

Remarkable progress has been witnessed within a recent decade for the precision designing of a wide variety of cyclic polymers, owing to newly developed synthetic means, i.e., an end-to-end polymer linking process,[1−3] as well as an alternative ring-expansion polymerization.[4−9] And by making use of diverse cyclic polymers of the prescribed chemical compositions, remarkable topology effects have now been disclosed either by the elimination of chain ends of linear polymers, leading to their conformational constriction in comparison with their linear and branched counterparts.[10−12]

Notably, in particular, cyclic polymers having densely appended functional groups could provide a unique opportunity to attain amplified topology effects through the accumulation of the interaction between pendant functional groups, as reported in cyclic graft copolymers.[13−18] Accordingly, we have newly prepared a pair of topologically contrastive, linear and cyclic polymers having densely appended perylene diimide (PDI) units, to explore any topology effects in their thin-film electron carrier mobility. A class of *linear* polymers having pendant PDI units of unique physico- and electrochemical properties[19] have been a subject of extensive studies, covering their photophysical properties,[20,21] microphase separation,[22] and electrophysical characteristics.[23] Besides, the thin-film electron carrier mobility is of an particular interest in the fabrication of optoelectronic devices, like organic solar cells and organic light-emitting devices.[24,25] Though the electron carrier mobility property is known to be tunable either through the molecular designing, the π-extension by the polymerization of semiconducting units, or crystallization/self-assembly techniques,[26−28] an alternative means to tune the device performance could be realized by the polymer topology effects with cyclic/cyclized polymers.

In the present study, we have employed an electrostatic self-assembly and covalent fixation (ESA-CF) process[10,29] to prepare a pair of linear and cyclic polymers having pendant PDI units at each monomer repeating unit of backbone chain, **IV_L** and **IV_C**, for the subsequent thin-film electron mobility measurements.[30] The ESA-CF technique has so far been applied to the precision syntheses of complex polymer topologies, including monocyclic/multicyclic polymers[10] and comb-shaped polymers,[31,32] as well as to the surface modification of solids and fabrics.[33] The ESA-CF process is now demonstrated to afford a pair of linear and cyclic polymers having defined backbone segment length, and having densely appended bulky PDI units, in order to explore topology effects on their thin film electron carrier mobility measured by the electron-only device (EOD).

RESULTS AND DISCUSSION

Preparation of Linear and Cyclic Poly(perylene diimide acrylate) (IV$_L$ and IV$_C$). A pair of linear and cyclic polymers having pendant perylene diimide (PDI) units at each

Received: June 7, 2016
Revised: July 28, 2016
Published: August 5, 2016

DOI: 10.1021/acs.macromol.6b01225
Macromolecules 2016, 49, 5831−5840

Scheme 1. Preparation of Linear and Cyclic Poly(sodium acrylate)s

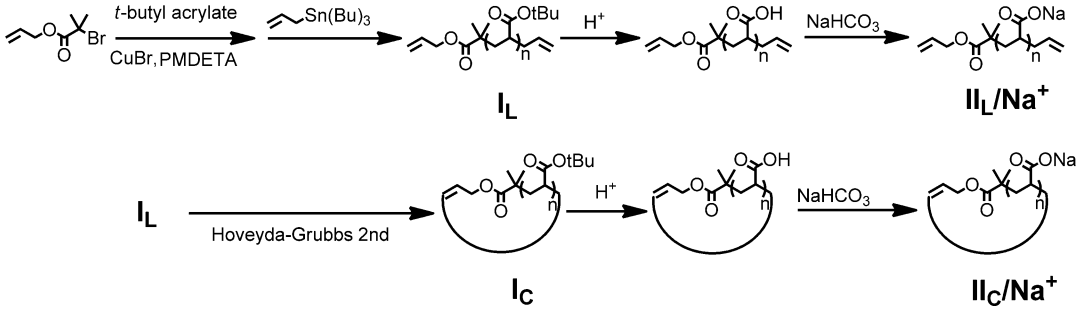

monomer repeating unit of backbone chain, $\mathbf{IV}_L$ and $\mathbf{IV}_C$, have been prepared by the ESA-CF process, by using an anionic component of linear and cyclic poly(sodium acrylate), $\mathbf{II}_L/\mathbf{Na}^+$ and $\mathbf{II}_C/\mathbf{Na}^+$, respectively, having different segment lengths, and a cationic component of a perylene diimide (PDI) derivative having a cyclic ammonium salt group, $\mathbf{III}/\mathbf{TfO}^-$.

As a first step, a pair of linear and cyclic poly(sodium acrylate) of different segment lengths were prepared. Thus, a series of telechelic poly(*tert*-butyl acrylate)s having allyl end groups and of three different molecular weights ($\mathbf{I}_L$-**1**, $\mathbf{I}_L$-**2**, and $\mathbf{I}_L$-**3**) were produced through an atom transfer radical polymerization (ATRP)[34] of *tert*-butyl acrylate with an initiator having an allyl group, followed by the end-capping reaction with allyltributylstannane.[35] The subsequent ring-closing metathesis reactions of a series of $\mathbf{I}_L$ were performed in the presence of Hoveyda−Grubbs catalyst second generation under dilution, to afford the corresponding cyclic poly(*tert*-butyl acrylate)s, ($\mathbf{I}_C$-**1**, $\mathbf{I}_C$-**2**, and $\mathbf{I}_C$-**3**) in 63−67% yields after the column purification to remove unreacted precursor as well as unassigned side products (Scheme 1).

A series of the cyclized products, $\mathbf{I}_C$, and their linear precursors, $\mathbf{I}_L$, were characterized by means of ^{1}H NMR, MALDI TOF mass, and SEC techniques. The ^{1}H NMR (Figure 1) showed the signals due to allyl protons at 4.94−5.36 and 5.61−6.01 ppm in $\mathbf{I}_L$, which were replaced after the cyclization by those due to inner olefin protons at 5.40−5.69 ppm in $\mathbf{I}_C$. The MALDI-TOF mass spectra of $\mathbf{I}_L$-**1** and $\mathbf{I}_C$-**1** (Figure 2) showed commonly a uniform series of peaks derived from poly(*tert*-butyl acrylate) (peak interval of 128 mass units), and each peak exactly matched to theoretically calculated mass values. And, the difference of the corresponding molar mass of $\mathbf{I}_L$ ((4036.5 − $[Na]^+$) = 4013.5) and that of $\mathbf{I}_C$ ((4009.1 − $[Na]^+$) = 3986.1), both with DP_n of 30, equals 27.4, in accord with the elimination of an ethylene molecule (molecular weight of C_2H_4 = 28.05). Furthermore, the SEC comparison of a set of the linear ($\mathbf{I}_L$-**1**, -**2**, and -**3**) and the cyclized ($\mathbf{I}_C$-**1**, -**2**, and -**3**) products (Figure S1) showed that the cyclized products $\mathbf{I}_C$ maintained nearly symmetrical elution profiles as in the linear precursors, $\mathbf{I}_L$, and the apparent peak molecular weights, corresponding to the hydrodynamic volume, were marginally smaller (0.77−0.81) than those of linear counterparts, $\mathbf{I}_L$, indicative of the effective polymer cyclization to proceed.

The subsequent acid hydrolysis of *tert*-butyl ester groups in $\mathbf{I}_L$ and in $\mathbf{I}_C$ was completed by the treatment with trifluoroacetic acid, and the following neutralization with sodium hydrogen carbonate produced a pair of linear and cyclic poly(sodium acrylate)s ($\mathbf{II}_L/\mathbf{Na}^+$ and $\mathbf{II}_C/\mathbf{Na}^+$, respectively). It was confirmed by ^{1}H NMR inspection (Figure S2) that the chain-end or the in-chain allyl ester groups were retained intact

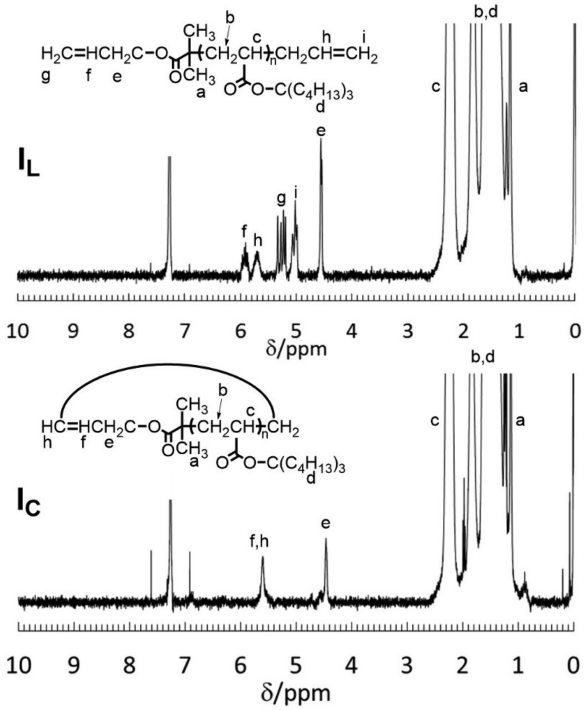

Figure 1. ^{1}H NMR spectra of (top) linear and (bottom) cyclic poly(*tert*-butyl acrylate)s (300 MHz, $CDCl_3$, 25 °C).

during the applied acid treatment to remove *tert*-butyl ester groups in $\mathbf{I}_L$ and in $\mathbf{I}_C$ (Scheme 1).

For the preparation of a cationic PDI derivative having a 5-membered *N*-phenylpyrrolidinium group, $\mathbf{III}/\mathbf{TfO}^-$, on the other hand, the two-step conversion of a PDI derivative having a hydroxyl group[36] was carried out, namely, the treatment with triflic anhydride to form a PDI derivative having a triflate ester group, followed by the quaternization with *N*-phenylpyrrolidine[37] (Scheme 2).

The isolated $\mathbf{III}/\mathbf{TfO}^-$ was characterized by means of ^{1}H NMR and MALDI-TOF mass spectroscopic techniques (Figures 3 and 4, respectively). The ^{1}H NMR showed the signals due to *N*-phenylpyrrolidinium salt groups at 3.77−4.45 ppm together with those due to perylene aromatic group at 8.03−8.64 ppm. The MALDI-TOF mass showed a peak at m/z = 803.41, corresponding to the most abundant mass of the cationic product, $\mathbf{II}^+$, possessing the expected chemical structure of $C_{53}H_{60}N_3O_4$ of 803.08, with removing a triflate anion.

The ESA-CF method has so far been applied to produce various comb polymers having densely appended graft polymer segments by employing anionic linear poly(sodium acrylate)

DOI: 10.1021/acs.macromol.6b01225
Macromolecules 2016, 49, 5831−5840

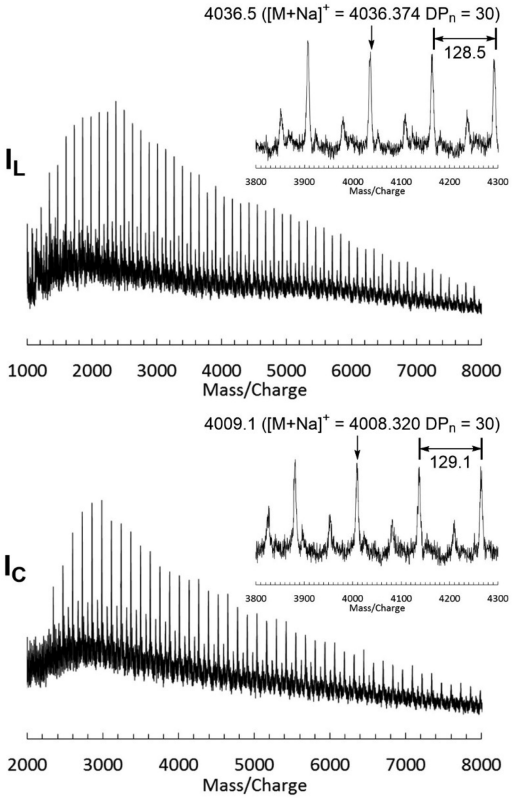

Figure 2. MALDI-TOF mass spectra of (top) linear and (bottom) cyclic poly(*tert*-butyl acrylate)s (linear mode, dithranol with sodium trifluoroacetate as a matrix). DP_n denotes the number of monomer units in the products. Minor series of peaks with the mass difference of 57 from the main peaks are assignable to the product formed by the elimination of one *tert*-butyl unit.

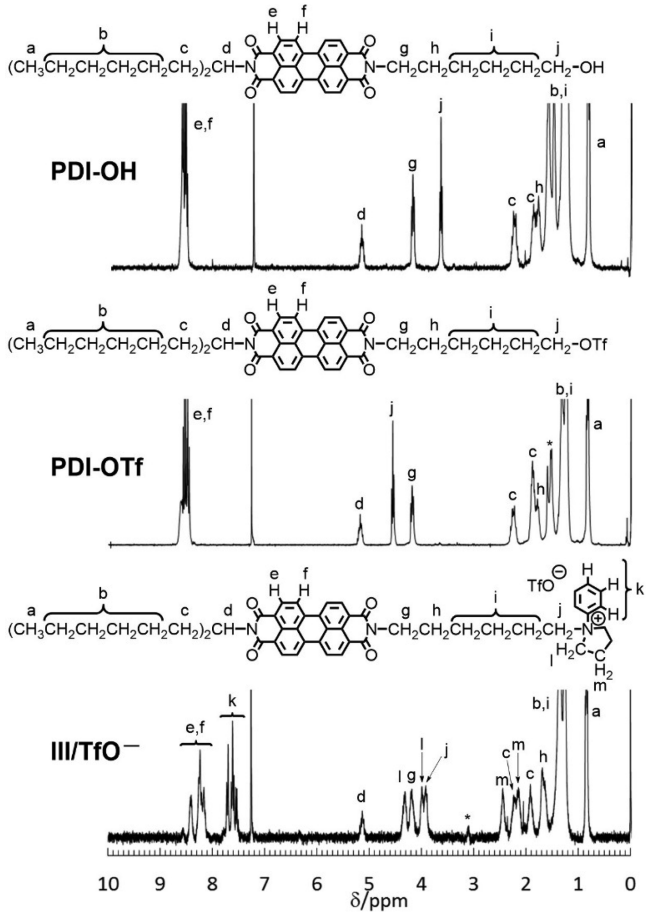

Figure 3. ^{1}H NMR spectra of PDI derivatives having (top) a hydroxyl group, (middle) a triflate ester group, and (bottom) a 5-membered cyclic quaternary salt group, **III**/**TfO**$^-$ (300 MHz, $CDCl_3$, 25 °C).

and cationic poly(THF)s having a cyclic ammonium salt group.[31,32] A simple precipitation treatment of the water-insoluble latter precursor into an aqueous solution containing the former precursor could promote the ion-exchange reaction by eliminating sodium triflate into aqueous medium. And in the ionic self-assembly by the prepolymer pair, the electrostatic interaction between the backbone and the graft components could overcome the steric repulsion between the polymeric reagents. Consequently, the comb-shaped polymer products were effectively produced after the covalent conversion by the ring-opening reaction of cyclic ammonium salt groups by carboxylate anions along the polymer backbone.[31,32]

Thus, in the present study, the precipitation treatment was conducted with an acetone solution of the cationic PDI precursor, **III**/**TfO**$^-$, into an aqueous solution containing an ionically equivalent amount of polyacrylate anion as a sodium salt form (**II**$_L$/**Na**$^+$ and **II**$_C$/**Na**$^+$, respectively) (Scheme 3). The self-assembly products, **II**$_L$/**III** and **II**$_C$/**III**, were subsequently recovered by the filtration. The nearly quantitative (88−98%) ion-exchange yields were then confirmed by the UV (526 nm) analysis after adding triflic acid to the weighed amount of the products, **II**$_L$/**III** and **II**$_C$/**III**, by reference to the regenerated cationic PDI precursor, **III**/**TfO**$^-$.

Scheme 2. Preparation of a PDI Derivative Having a Five-Membered Cyclic Ammonium Salt Group

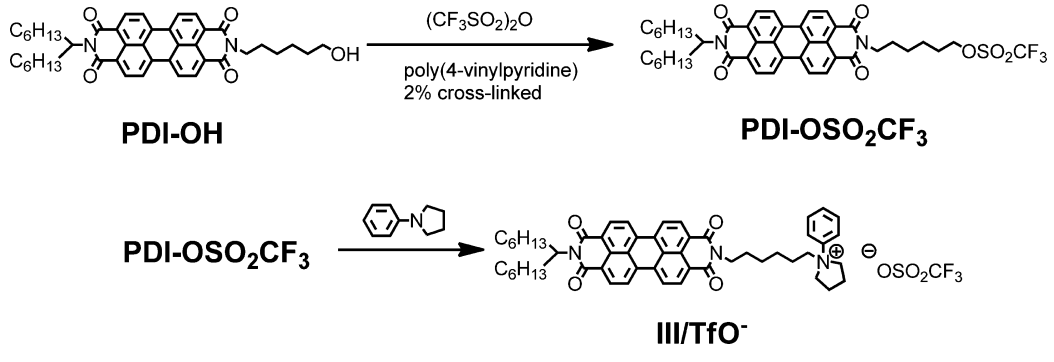

DOI: 10.1021/acs.macromol.6b01225
Macromolecules 2016, 49, 5831−5840

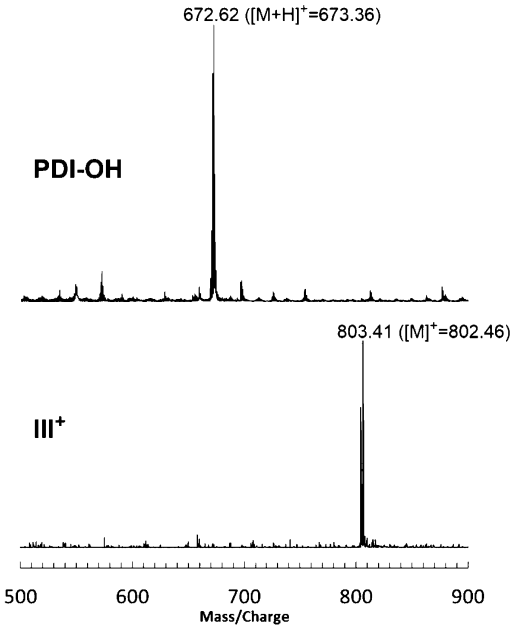

Figure 4. MALDI-TOF mass spectra of PDI derivatives having (top) a hydroxyl group and (bottom) a 5-membered cyclic quaternary salt group, **III**/TfO^- (linear positive ion mode, dithranol as a matrix).

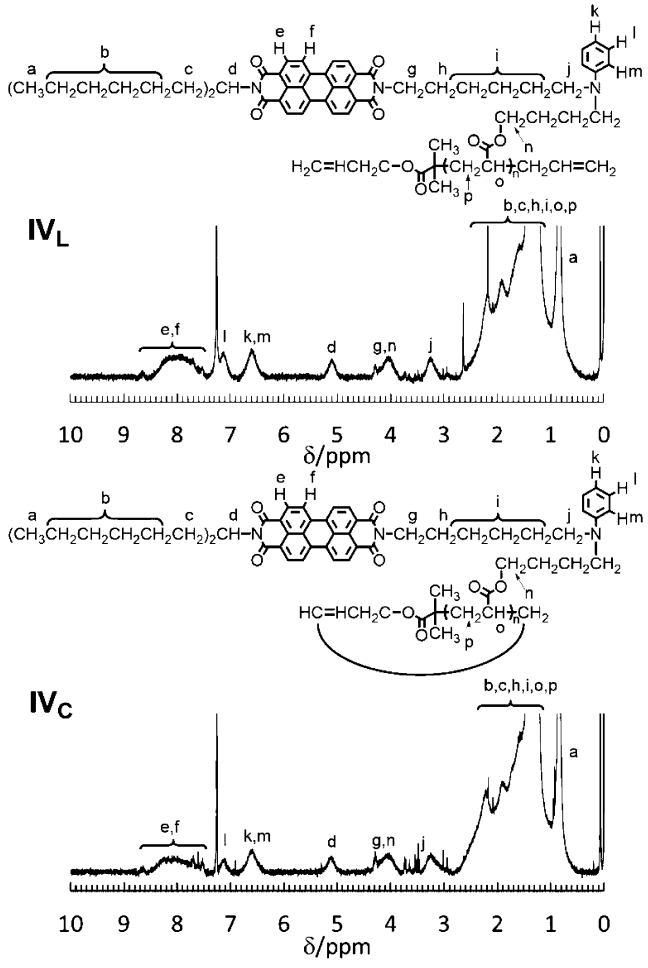

Figure 5. ^1H NMR spectra of (top) linear and (bottom) cyclic polymers having densely appended PDI units (300 MHz, $CDCl_3$, 25 °C).

Finally, the covalent conversion reactions of a pair of ionic precursors, $\mathbf{II}_L$/**III** and $\mathbf{II}_C$/**III**, were performed in dimethylacetamide at 180 °C for 12 h, to cause the ring-opening reaction of pyrrolidinium salt groups by acrylate anions. Thus, the higher temperature and prolonged reaction time were required to complete the covalent conversion in the present process in comparison with the relevant ESA-CF procedures so far reported.[10] The crude product, recovered after the precipitation into acetone, was subsequently subjected to the biobeads column chromatography to remove any ionic side products including the low molecular weight unreacted PDI or polymeric precursors. The dark-red solid products $\mathbf{IV}_L$ and $\mathbf{IV}_C$ were finally isolated in 12−19% yields.

The ^1H NMR of the covalent product $\mathbf{IV}_L$ and $\mathbf{IV}_C$ (Figure 5) confirmed the ring-opening reaction of the *N*-phenylpyrrolidinium salt groups by the carboxylate anion to proceed. Thus, the *N*-phenyl proton signal for the ionic self-assembly **II**/**III** at 7.48−7.85 ppm shifted toward 6.30−6.87 and 6.95−7.24 ppm, and the *N*-methylene proton signal newly appeared at around 3.2 ppm, to coincide with the ring-opening reaction of *N*-phenylpyrrolidinium salt groups by the acrylate anion. In addition, the IR analysis (Figure S3) showed that the triflate absorptions visible at 1224, 1030, and 637 cm^{-1} in **III**/TfO^- were removed after the ion-exchange treatment, and the ester absorption at 1730 cm^{-1} became visible after the covalent conversion process. Upon these characterization results, the formation of a pair of linear and cyclic polymers having densely appended perylene diimide (PDI) units $\mathbf{IV}_L$ and $\mathbf{IV}_C$ were unequivocally confirmed.

Scheme 3. ESA-CF Preparation of Linear and Cyclic Polymers Having Densely Appended PDI Units

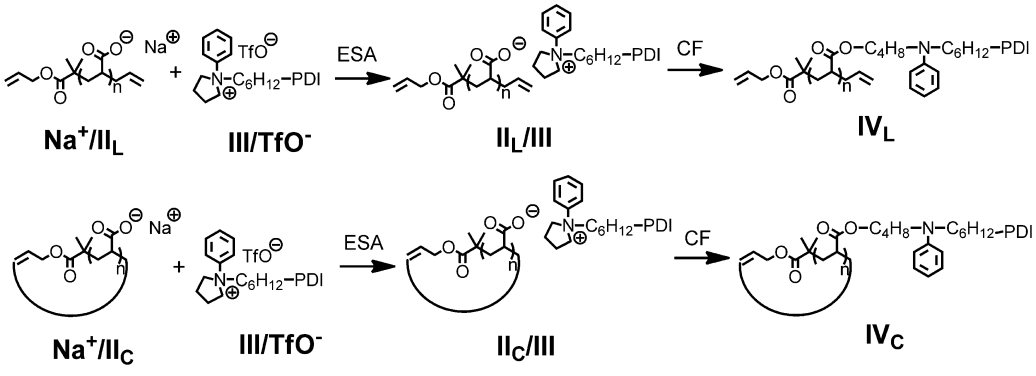

DOI: 10.1021/acs.macromol.6b01225
Macromolecules 2016, 49, 5831−5840

Self-Assemblies by Linear and Cyclic Poly(perylene diimide acrylate) (IV_L and IV_C). As both of linear and cyclic polymers having densely appended PDI units, IV_L and IV_C, could commonly form self-assembled structures through the $\pi-\pi$ stacking interaction between PDI units, the viscosity measurements were conducted in $CHCl_3$ solution to observe any distinction between the linear and the cyclic polymers IV_L and IV_C having various DP_n's.

As seen in Figure 6, a series of cyclic products IV_C exhibited constantly lower viscosities in comparison with their linear

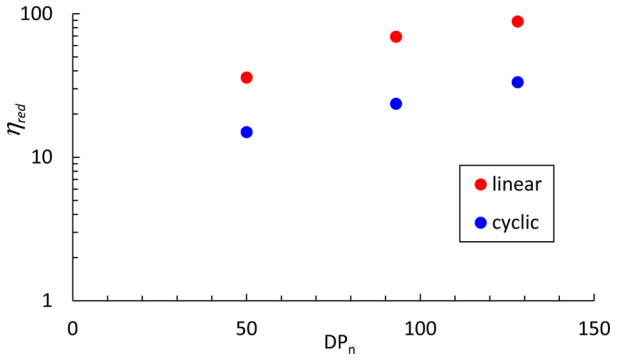

Figure 6. Reduced viscosity of (red) linear and (blue) cyclic polymers having densely appended PDI units with different DP_n's ($CHCl_3$, 2.0 g/L).

counterparts IV_L, to imply the suppression of the intermolecular interaction between PDI units in the cyclic polymers IV_L, as observed in a variety of supramolecular systems.[38] SEC measurements of a series of IV_L and IV_C, on the other hand, were circumvented by the anomalous elution behavior (Figure S4),[39] presumably due to the dynamic dissociation/association of the products IV_L and IV_C under the SEC conditions. UV−vis spectroscopic measurements on IV_L and IV_C (Figure S5) showed commonly a minor red-shifts of 2−5 nm against the monomeric precursor, **III**/TfO^-,[40] while any noticeable topology and segment length effects were not visible.

The TEM measurements were then conducted by the drop-casting of $CHCl_3$ solutions of IV_L and IV_C samples, and the results are collected in Figure 7. For IV_L-**1** and IV_C-**1** having the shortest backbone segments, dot-like aggregates of the several dozen nanometer sizes were observed together with spherical self-assemblies of a few hundred nanometers size (Figure 7, A and E). And for IV_L-**2** and IV_C-**2**, and for IV_L-**3** and IV_C-**3** having the longer backbone segments, spherical self-assemblies of one to five hundred nanometer sizes were commonly observed with their increasing populations along with the increase of the backbone segment length. (Figure 7, B and F, C and G, respectively) The optical microscope observation of the IV_L-**3** and IV_C-**3** (Figure 7, D and H) showed also the similar self-assemblies as observed in the TEM measurements. These results forming spherical assembly structures accord with the intermolecular association by pendant PDI units against the backbone segment with a spacer alkyl group, while noticeable distinction was not observed among the linear and cyclic samples between IV_L and IV_C.

Thin-Film Electron Mobility of Linear and Cyclic Poly(perylene diimide acrylate) (IV_L and IV_C). A pair of linear and cyclic polymers having pendant PDI units, IV_L and IV_C, were subsequently subjected to the thin film electron mobility measurements by means of an electron-only device, EOD, fabricated according to the previous reports[41,42] (Figure 8). Thus, either of the IV_L or IV_C sample in a $CHCl_3$ solution

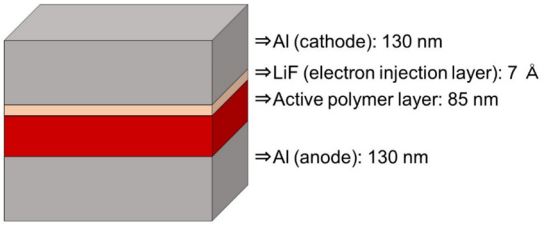

Figure 8. A layer structure of the electron-only device.

was spin-coated to form an active polymer layer on an aluminum anode layer, which was deposited upon an indium

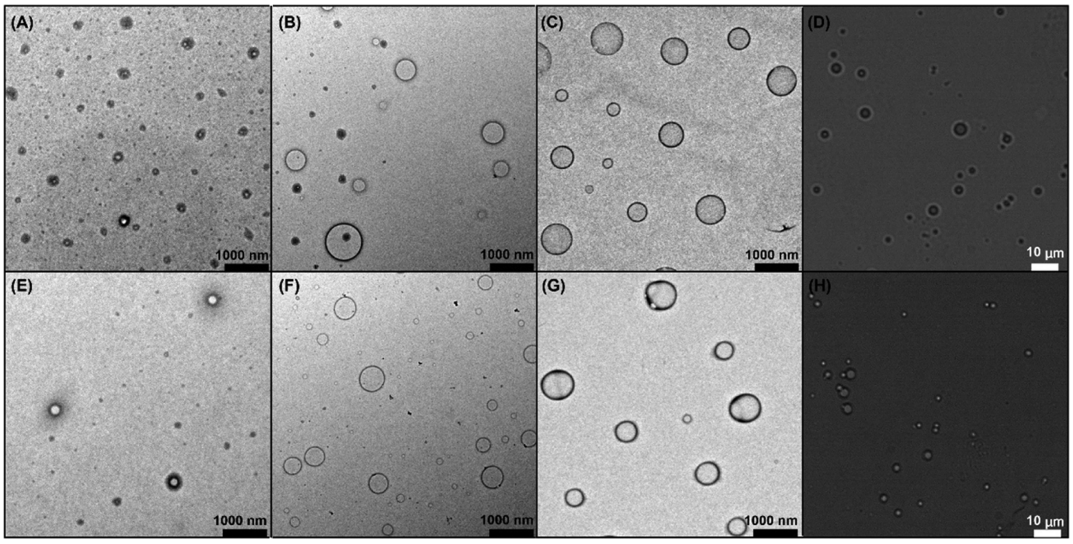

Figure 7. TEM images of linear polymers having densely appended PDI units with DP_n of (A) 50, (B) 93, and (C) 128 and of cyclic polymers having densely appended PDI units with DP_n of (E) 50, (F) 93, and (G) 128, and optical microscope images of (D) a linear polymer having densely appended PDI units with DP_n of 128 and of (H) a cyclic polymer having densely appended PDI units with DP_n of 128.

DOI: 10.1021/acs.macromol.6b01225
Macromolecules 2016, 49, 5831−5840

tin oxide (ITO)-coated glass substrate by the thermal evaporation. In order to maintain the polymer layer thickness of 85 nm for both from $\mathbf{IV}_L$ and $\mathbf{IV}_C$ samples, the higher concentration solution was used for the latter, $\mathbf{IV}_C$, in the present device fabrication process. After annealing at 80 °C, an electron injection lithium fluoride layer and a hole blocking aluminum cathode layer were further laminated. The fabricated EODs with three pairs sets of $\mathbf{IV}_L$ and $\mathbf{IV}_C$ were subjected to the $J-V$ characteristics measurements at least three times to confirm the data reproducibility.

The results of $J-V$ characteristics measurement are listed in Figure 9, and the electron mobility values obtained with a series

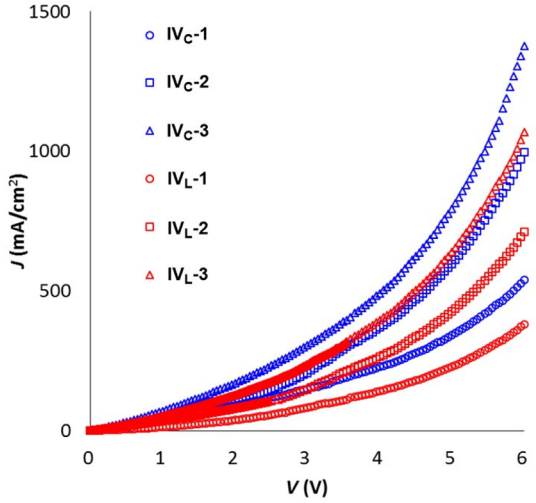

Figure 9. $J-V$ relationship for (red ○, □, △) linear and (blue ○, □, △) cyclic polymers having densely appended PDI units with DP_n of (red ○, blue ○) 50, (red □, blue □) 93, and (red △, blue △) 128.

of linear and cyclic polymers, $\mathbf{IV}_L$ and $\mathbf{IV}_C$, as the active layer, are collected in Table 1. The electron mobility was observed to increase monotonously along with the increase of the chain length not only for the linear polymers,[43] but also for the cyclic counterparts. Remarkably, moreover, the electron mobility with the cyclic $\mathbf{IV}_C$ was constantly higher than those with the linear counterparts $\mathbf{IV}_L$, while the margin (C/L in Table 1) was

Table 1. Results of Electron Carrier Mobility and Thin Film Density Measurements of Linear and Cyclic Polymers Having Densely Appended PDI Units with Different DP_n's

sample[a]		electron mobility[b]		film density			
					QCM/microfigure[d]		
code	DP_n		C/L[e]	XRR[c]	C/L[e]		C/L[e]
$\mathbf{IV}_L$-1	50	2.73	1.21	0.95	1.21	0.94	1.23
$\mathbf{IV}_C$-1	50	3.29		1.15		1.16	
$\mathbf{IV}_L$-2	93	3.56	1.16	0.92	1.20	0.89	1.28
$\mathbf{IV}_C$-2	93	4.12		1.10		1.14	
$\mathbf{IV}_L$-3	128	4.25	1.10	0.95	1.15	0.95	1.22
$\mathbf{IV}_C$-3	128	4.67		1.09		1.16	

[a]See Scheme 3 for sample details. [b]Measured by the EOD device, in $cm^2/(V\ s)$ ($\times 10^{-4}$). [c]Measured by the XRR method, in g/cm^3. [d]Meaured by the QCM/microfigure technique, in g/cm^3. [e]The ratios of $\mathbf{IV}_L$-1 and $\mathbf{IV}_C$-1, $\mathbf{IV}_L$-2 and $\mathbf{IV}_C$-2, and $\mathbf{IV}_L$-3 and $\mathbf{IV}_C$-3.

reduced from 1.21 to 1.10 along with the increase of the backbone chain length, DP_n.

Furthermore, the thin film density of a series of linear and cyclic polymers, $\mathbf{IV}_L$ and $\mathbf{IV}_C$, was measured by means of the two independent techniques, namely the X-ray reflectometer (XRR) and by the combined quartz crystal microbalance (QCM)/microfigure techniques. The XRR measurement was performed with polymer film samples prepared by the spin-coating technique relevant to the EOD fabrication procedure (Figure S6). The film density data were obtained subsequently through the extrapolation of simulated fitting curves, as previously applied for organic thin films samples,[44] where a "genetic algorithm" fitting program was applied. The combined QCM/microfigure measurement was also employed to determine the thin-film density of the polymer samples, where the polymer thin films were again prepared by the spin-coating on quartz resonator, to determine the weight of the deposited polymer film based on the variation of frequency.[45] And the additional microfigure measurements allowed to determine the height of the deposited polymer film. From these combined measurements, the density of the polymer thin films was determined.

The results of the thin film density of a series of linear and by the cyclic polymers, $\mathbf{IV}_L$ and $\mathbf{IV}_C$, are also listed in Table 1, to compare with their electron carrier mobility. The thin-film density values by the two independent methods were in a good agreement each other and, remarkably, were higher for the cyclic $\mathbf{IV}_C$ in comparison with the linear counterparts $\mathbf{IV}_L$ (from 1.15 to 1.21 times by XRR and from 1.22 to 1.28 times for the combined QCM/microfigure method, respectively). On the other hand, the backbone polymer segment lengths, DP_n, of either $\mathbf{IV}_L$ or $\mathbf{IV}_C$ were not noticeably affected on their thin film density, in contrast to their electron carrier mobility affected thereby.

Moreover, grazing-incidence wide-angle X-ray scattering (GIWAXS) measurements were carried out in order to investigate microstructures of the thin films (e.g., polymer crystallinity and packing orientations). The obtained GIWAXS patterns (Figure S7) showed the absence of any clear $\pi-\pi$ stacking structure (generally the peaks appear around $q \sim 1.8$ $Å^{-1}$) in all the thin film samples. On the other hand, the increased density listed in Table 1 implies the enhanced aggregation of polymer chains in the thin films of cyclic polymers compared to that of linear polymers. It is thus supposed that the enhanced aggregation for the cyclic polymer thin films should be responsible for the enhancement in the electron mobility.

In summary, the present study showed first that the ESA-CF process is an effective means to produce a pair of linear and cyclic polymers having densely appended PDI units and subsequently demonstrated that the topology (cyclic or linear) of backbone segment, or the presence or the absence of the end groups in electron-conducting polymers, $\mathbf{IV}_L$ and $\mathbf{IV}_C$, decisively affects their electron carrier mobility, in relation to their thin film density at their self-assembly states. The current findings show a new topology effect arisen from the elimination of end groups of the linear functional polymers to promise future application potentials in electronics/photonics area and beyond.

EXPERIMENTAL SECTION

Materials. A perylene diimide derivative having a hydroxyl group (Scheme 2) was prepared according to the method reported before.[36]

DOI: 10.1021/acs.macromol.6b01225
Macromolecules 2016, 49, 5831−5840

N-Phenylpyrrolidine was obtained by the procedure described before.[46] Trifluoromethansulfonic anhydride (triflic anhydride) (98%, Nacalai Tesque, Inc.) was distilled over P_2O_5 just before use. Toluene (99.0%, Kanto Chemical Co., Inc.) and dichloromethane (99.0%, Kanto Chemical Co., Inc.) were distilled over CaH (Nacalai Tesque, Inc.). Poly(4-vinylpiridine), 2% cross-linked with divinylbenzene (Aldrich), was washed with hexane and $CHCl_2$ and heated 60 °C under vacuum for more than 6 h before use. Allyl-2-bromo-2-methylpropionate (98%, Aldrich), *N*,*N*,*N*′,*N*″,*N*″-pentamethyldiethylenetriamine (PMDETA) (>98.0% Tokyo Chemical Industry Co., Ltd.), *tert*-butyl acrylate (>98.0% Tokyo Chemical Industry Co., Ltd.), allyltributylstannane (97%, Aldrich), CuBr (99%, Nacalai Tesque, Inc.), trifluoroacetic acid (>98.0%, Wako Pure Chemical Industries, Ltd.), magunesium sulfate, anhydrous (>98.0%, Kanto Chemical Co., Inc.), sodium hydrogen carbonate (>99.0%, Kanto Chemical Co., Inc.), siliamets DMT (SiliCycle Inc.), Hoveyda–Grubbs catalyst second generation (97%, Aldrich), and ethyl vinyl ether (>99%, Aldrich) were used as received. Wakosil C-300 (Wako Pure Chemical Industries, Ltd.) and aluminum oxide, activated (>90%, Wako Pure Chemical Industries, Ltd.) were used as received for flash chromatography. Biobeads S-X1 Support (Bio-Rad Laboratories, Inc.) was washed with chloroform and was swelled 24 h before use. LiF (>99.99%, Aldrich) and Al (Furuuchi Chemical Co.) were used as received for vacuum deposition.

Preparation of Linear Poly(*tert*-butyl acrylate) Having Allyl End Groups (I_L-1, -2, and -3). The preparation of poly(*tert*-butyl acrylate) having olefinic end groups was carried out through an atom transfer radical polymerization (ATRP) technique.[34] Thus, a weighed amount of *tert*-butyl acrylate (30 mL), purified by passing through an alumina column, was mixed with CuBr (146.4 mg), *N*,*N*,*N*′,*N*″,*N*″-pentamethyldiethylenetriamine (276 μL), and allyl-2-bromo-2-methylpropionate (162 μL) in a flask under nitrogen. The reaction solution was subjected to the repeated freeze–pump–thaw treatment and heated to 110 °C for the prescribed time (15, 30, or 45 min). The reaction solution was then rapidly cooled to 0 °C, and the residual monomer was removed under the reduced pressure. Thereupon, allyltributylstannane (1.58 mL) in toluene (30 mL) was injected, followed by the freeze–pump–thaw treatment. The mixture solution was again heated to 110 °C for 16 h to proceed the reaction. After the solvent was removed under reduced pressure, the concentrated solution was passed through a plug of alumina with $CHCl_3$ and of silica gel first with acetone and then with $CHCl_3$. Finally, the product was subjected to a preparative SEC technique to remove the low molecular weight side products to give a series of polymer products, **I_L-1** (3.33 g, M_n(NMR) = 6500, M_p(SEC) = 7400, $Đ_M$ = 1.28), **I_L-2** (5.12 g, M_n(NMR) = 12 100, M_p(SEC) = 12 800, $Đ_M$ = 1.22), and **I_L-3** (7.57 g, M_n(NMR) = 16 400, M_p(SEC) = 17 500, $Đ_M$ = 1.19). ^{1}H NMR (300 MHz, $CDCl_3$, 25 °C, TMS): δ 1.07–2.02 (m, $-CH_2CHCOO-$), 2.07–2.54 (m, $-CH_2CHCOO-$, $-C(CH_3)_3$), 4.49–4.63 (m, 2H; $-OCH_2CH=CH_2$), 4.94–5.13 (m, 2H; $-CH_2CH=CH_2$), 5.17–5.37 (m, 2H; $-OCH_2CH=CH_2$), 5.61–5.80 (m, 1H; $-CH_2CH=CH_2$), 5.85–6.01 (m, 1H; $-OCH_2CH=CH_2$).

Synthesis of Cyclic Poly(*tert*-butyl acrylate) (I_C-1, -2, and -3). A weighed amount of either **I_L-1**, **-2**, or **-3** (250 mg) and Hoveyda–Grubbs catalyst second generation (104.5 mg) were mixed in toluene (1 L) under nitrogen. The resulting reaction solution (0.25 g/L) was heated at 80 °C for 48 h in the dark. Thereafter, an excess amount of ethyl vinyl ether (15 mL) was added to stir for another 0.5 h. After removing the solvent by the evaporation, the residual reaction mixture was treated first by an alumina column chromatography with $CHCl_3$, followed by a silica gel column chromatography first with $CHCl_3$ and then with acetone. The crude product was recovered by evaporating the solvent and was subjected to a preparative SEC fractionation technique to remove the low molecular weight impurities. Finally, the recovered product was dissolved in a small amount of $CHCl_3$, and treated with a catalyst scavenger, SiliaMetS(R), for 1 h to give **I_C-1** (167.3 mg, 67% yield, M_n(NMR) = 6400, M_p(SEC) = 5700, $Đ_M$ = 1.38), **I_C-2** (158.7 mg, 63% yield, M_n(NMR) = 21 400, M_p(SEC) = 10 400, $Đ_M$ = 1.26), and **I_C-3** (159.7 mg, 64% yield, M_n(NMR) = 34 600, M_p(SEC) = 13 900, $Đ_M$ = 1.25). ^{1}H NMR (300 MHz, $CDCl_3$, 25 °C, TMS): δ 1.08–1.94 (m, $-CH_2CHCOO-$), 2.06–2.58 (m, $-CH_2CHCOO-$, $-C(CH_3)_3$), 4.38–4.53 (m, 2H; $-OCH_2CH=CH-$), 5.40–5.69 (m, 2H; $=CH-$).

Synthesis of Linear and Cyclic Poly(sodium acrylate) (II_L/Na^+-1, -2, and -3, II_C/Na^+-1, -2, and -3). The obtained linear and cyclic poly(*tert*-butyl acrylate)s, I_L and I_C, were then treated with trifluoroacetic acid (10 times molar excess of the repeating acrylate units) in dehydrated dichloromethane (20 mL) at ambient condition for 24 h under stirring. After evaporating the solvent, the residual product was again dissolved in methanol and filtrated to remove insoluble side products. The evaporation of the solvent gave the poly(acrylic acid) products, **II_L/H^+-1** (88.2 mg, 79% yield), **II_L/H^+-2** (98.0 mg, 88% yield), **II_L/H^+-3** (96.2 mg, 86% yield), **II_C/H^+-1** (80.1 mg, 86% yield), **II_C/H^+-2** (74.0 mg, 83% yield), and **II_C/H^+-3** (84.6 mg, 75% yield). ^{1}H NMR of **II_L/H^+** (300 MHz, CD_3OD, 25 °C): δ 1.06–1.23 (m, 6H; $-CH_3$), 1.34–2.11 (m, $-CH_2CHCOO-$), 2.17–2.58 (m, $-CH_2CHCOO-$), 4.44–4.60 (m, 2H; $-OCH_2CH=CH_2$), 4.90–5.13 (m, 2H; $-CH_2CH=CH_2$), 5.17–5.35 (m, 2H; $-OCH_2CH=CH_2$), 5.65–5.82 (m, 1H; $-CH_2CH=CH_2$), 5.84–6.01 (m, 1H; $-OCH_2CH=CH_2$). ^{1}H NMR of **II_C/H^+** (300 MHz, CD_3OD, 25 °C): δ 0.95–1.15 (m, 6H; $-CH_3$) 1.29–2.01 (m, $-CH_2CHCOO-$), 2.10–2.48 (m, $-CH_2CHCOO-$), 4.33–4.44 (m, 2H; $-OCH_2CH=CH-$), 5.47–5.71 (m, 2H; $=CH-$). A weighed amount of the obtained poly(acrylic acid) product, **II_L/H^+** or **II_C/H^+** was dissolved in a small amount of methanol. Thereupon, an aqueous sodium hydrogen carbonate solution was added dropwise under stirring to reach the solution pH to 7, and the reaction was allowed to proceed for further 12 h. After evaporating the solvent, the poly(sodium acrylate) products were subjected to the dialysis treatment against pure water. **II_L/Na^+-1** (95.7 mg, 84% yield), **II_L/Na^+-2** (99.1 mg, 78% yield), **II_L/Na^+-3** (134.8 mg, 93% yield), **II_C/Na^+-1** (95.7 mg, 93% yield), **II_C/Na^+-2** (91.5 mg, 96% yield), and **II_C/Na^+-3** (95.0 mg, 96% yield). ^{1}H NMR of **II_L/Na^+** (300 MHz, D_2O, 25 °C): δ 0.89–1.01 (m, 6H; $-CH_3$), 1.04–1.65 (m, $-CH_2CHCOO-$), 1.65–2.22 (m, $-CH_2CHCOO-$), 3.38–3.53 (m, 2H; $-OCH_2CH=CH_2$), 4.98–5.18 (m, 2H; $-OCH_2CH=CH_2$), 5.49–5.64 (m, 1H; $-CH_2CH=CH_2$), 5.67–5.86 (m, 1H; $-OCH_2CH=CH_2$). ^{1}H NMR of **II_C/Na^+** (300 MHz, D_2O, 25 °C): δ 0.90–1.09 (m, 6H; $-CH_3$) 1.09–1.66 (m, $-CH_2CHCOO-$), 1.66–2.26 (m, $-CH_2CHCOO-$), 3.42–3.56 (m, 2H; $-OCH_2CH=CH-$), 5.20–5.77 (m, 2H; $=CH-$).

Preparation of a PDI Derivative Having a Pyrrolidinium Salt Group (III/TfO^-). A weighed amount of a perylene diimide derivative having a hydroxyl group (300 mg) was mixed with poly(4-vinylpyridine)–2% cross-linked (462 mg) in dehydrated dichloromethane (75 mL) under nitrogen. The reaction solution was then placed dry iced acetone bath at −78 °C, and triflic anhydride (435 μL) was injected rapidly. The reaction was allowed to proceed for 2 h under stirring, followed by the treatment with aqueous $NaHCO_3$. The separated organic phase was then dried by $MgSO_4$, and the solvent was removed by evaporation to give a triflate ester product (274 mg, 76% yield). The obtained triflate ester product was then dissolved in dehydrated dichloromethane (20 mL) under nitrogen at 0 °C. Thereupon, *N*-phenylpyrrolidine (245 μL) was added by a syringe to proceed the quaternization reaction for 1 h under stirring. The crude product, recovered by evaporating the solvent, was washed by hexane and by ethyl acetate to give the product, **III/TfO^-** (240 mg, 74% yield). ^{1}H NMR (300 MHz, $CDCl_3$, 25 °C): δ 0.84 (t, *J* = 6.6 Hz, 6H; $-CH_3$), 1.09–1.53 (m, 22H; $-(CH_3CH_2CH_2CH_2CH_2CH_2)_2C-$), 1.83–1.99 (m, 2H; $(-CH_2)_2CH-$), 2.09–2.19 (m, 2H; $-NArCH_2CH_2-$), 2.19–2.32 (m, 2H; $(-CH_2)_2CH-$), 2.32–2.54 (m, 2H; $-NArCH_2CH_2-$), 3.77–3.96 (m, 2H; $-NArCH_2-$), 3.96–4.05 (m, 2H; $-NArCH_2-$), 4.09–4.26 (m, 2H; $-NCH_2-$), 4.26–4.45 (m, 2H; $-NArCH_2-$), 5.03–5.23 (m, 1H; $-CH-$), 7.48–7.85 (m, 5H; NAr–*H*), 8.03–8.64 (m, 8H; Ar–*H*).

Preparation of Linear and Cyclic PPerAcr (IV_L -1, -2, and -3, IV_C-1, -2, and -3). Into an ice-cooled aqueous solution (50 mL) containing a weighed amount of **II_L/Na^+** or **II_C/Na^+** (10.0 mg, 0.105 mmol/repeating unit) was added dropwise an acetone solution (2.0

DOI: 10.1021/acs.macromol.6b01225
Macromolecules 2016, 49, 5831–5840

mL) of **III**/TfO^- (100 mg, 0.105 mmol) under vigorous stirring. The formed precipitate was collected by filtration after stirring 1 h and dried under reduced pressure. The product was finally isolated by the reprecipitation first with $CHCl_3$/methanol and then $CHCl_3$/acetone systems. In order to estimate the degree of the ion-exchange reaction, a weighed amount of the ion-exchanged product in $CHCl_3$ solution (0.2 g/L) was prepared under nitrogen, and an excess of trifluoromethanesulfonic acid was added. After 5 min with stirring, an aliquot of the resulting solution was subjected to the UV−vis measurement with the calibration using **III**/TfO^-. The ion-exchange yields were thus determined as 92% (**III**/II_L-**1**), 89% (**III**/II_C-**1**), 92% (**III**/II_L-**2**), 98% (**III**/II_C-**2**), 94% (**III**/II_L-**3**), and 88% (**III**/II_C-**3**).

The covalent conversion reaction of **III**/II_L and of **III**/II_C was performed as follows. Thus, the isolated product of **III**/II_L or **III**/II_C was dissolved in dimethylacetamide (20 mL) and was heated at 180 °C for 12 h. Thereafter, the solution was concentrated by removing most of the solvent under reduced pressure, and the residual mixture was poured into acetone to recover the precipitated product. The product was further purified by biobeads column to remove the unreacted PDI derivative and other ionic polymer products. IV_L-**1** (21.4 mg, 19% yield), IV_L-**2** (21.0 mg, 19% yield), IV_L-**3** (15.2 mg, 15% yield), IV_C-**1** (17.7 mg, 16% yield), IV_C-**2** (12.7 mg, 12% yield), and IV_C-**3** (14.3 mg, 14% yield). ^{1}H NMR of IV_L (300 MHz, $CDCl_3$, 25 °C, TMS): δ 0.33−0.99 (m, $-CH_3$), 0.98−2.71 (m, $-(CH_3CH_2CH_2-CH_2CH_2CH_2)_2CH-$, $-NCH_2CH_2CH_2CH_2CH_2CH_2N-$, $-CH_2CHCOO-$, $-CH_2CHCOO-$), 3.01−3.43 (m, $-NArCH_2-$), 3.82−4.36 (m, $-NCH_2-$, $-COOCH_2-$), 4.94−5.23 (m, $-CH-$), 6.30−6.84 (m, −NAr−*H* ortho and para to N), 6.98−7.21 (m, −NAr−*H* meta to N), 7.44−8.74 (m, Ar−*H*). ^{1}H NMR of IV_C (300 MHz, $CDCl_3$, 25 °C, TMS): δ 0.41−0.97 (m, $-CH_3$), 1.00−2.80 (m, $-(CH_3CH_2CH_2CH_2CH_2CH_2)_2CH-$, $-NCH_2CH_2CH_2-CH_2CH_2CH_2N-$, $-CH_2CHCOO-$, $-CH_2CHCOO-$), 2.90−3.44 (m, $-NArCH_2-$), 3.80−4.34 (m, $-NCH_2-$, $-COOCH_2-$), 4.91−5.32 (m, $-CH-$), 6.36−6.87 (m, −NAr−*H* ortho and para to N), 6.95−7.24 (m, −NAr−*H* meta to N), 7.44−8.76 (m, Ar−*H*).

Spectroscopic and Chromatographic Measurements. ^{1}H NMR spectra were recorded on a JEOL JNM-AL300 apparatus using $CDCl_3$, CD_3OD, or D_2O as a solvent. Proton chemical shifts (ppm) were referenced to the signal of tetramethylsilane. Size exclusion chromatography (SEC) measurements were performed using a Tosoh model CCPS equipped with a refractive index detector model RI 8200 and a UV detector model UV 8020 at 254 nm. As a SEC column, TSK G3000HXL was used with $CHCl_3$ as an eluent at a flow rate of 1.0 mL/min at 40 °C. MALDI-TOF mass spectra were recorded on a Shimadzu AXIMA-performance mass spectrometer equipped with a nitrogen laser (λ = 337 nm) and pulsed ion extraction. The spectrometer was operated at an accelerating potential of 20 kV with a linear-positive ion mode. For the measurement of a PDI sample, **III**/TfO^-, a $CHCl_3$ solution (1 mg/mL) and dithranol (20 mg/mL) were mixed (30/30 in μL). For the measurement of poly(*tert*-butyl acrylate) samples, on the other hand, a $CHCl_3$ solution (1 mg/mL), dithranol (20 mg/mL), and sodium trifluoroacetate (10 mg/mL) were mixed (30/100/70 in μL). A 3 μL portion of the mixture solution above was deposited onto a sample target plate. Mass values were calibrated by the four-point method using dendrimer calibrants, SpheriCal(Polymer Factory) Na^+ with a set of peaks at 732.82, 953.03, 1173.26, 1479.61, or at 1693.82, 2234.38, 2774.94, 3401.63, or at 3615.85, 4797.08, 5978.31, 7245.68 in tune with mass values of the measured compounds. Viscosity measurements were conducted with an Ostwald viscometer using a $CHCl_3$ solution at the concentration of 2.0 mg/mL and were repeated five times, and averaged data were reported. UV−vis measurements were performed with a JASCO V-670 spectrophotometer at 25 °C by using a sample solution. TEM measurements were conducted with a JEOL JEM-1010BS, using the film sample prepared by casting the solution on a carbon film supported by a copper grid. Optical microscope measurements were performed with an Olympus, BX51, by holding the sample solution between cover glass and a slide glass under 25 °C. For samples for the UV−vis, TEM, and optical microscopy measurements, a $CHCl_3$ solution at the concentration of 10 μg/mL was prepared and subjected to the filteration through a 0.2 μm pore membrane filter. Grazing-incidence wide-angle X-ray scattering (GIWAXS) measurements were carried out at BL45XU in SPring-8 (Hyogo, Japan). The wavelength of the X-ray beam was 0.1 nm, and the camera length was 395 mm. The 2D-scattering image was acquired using a photon counting detector (Pilatus3X 2M, Dectris Ltd.). The thin-film samples fabricated according to the reported procedure[41,42] were mounted in a helium cell to reduce radiation damage. A data acquisition time was 10 s. GIWAXS data were measured at the incident angle of 0.10°, which was lower than the critical angle of total external reflection at the substrate surface and was close to those of samples.

Fabrication of an Electron-Only Device and Electron Mobility Measurements. An electron-only device (EOD) was fabricated according to the reported procedure.[41,42] Thus, first, a 130 nm thickness Al layer was deposited on the quartz substrate coated with indium tin oxide (ITO) (Techno Print Co., Ltd.) by means of the thermal evaporation technique at the rate 6−7 Å/s. Then, a 85 nm thickness active polymer layer was formed by the spin coating of either with IV_L or with IV_C at 1000 rpm for 30 s, followed by the annealing at 80 °C for 30 min inside the globe box under argon. The spin coating solution concentration in dehydrated $CHCl_3$ was 10 mg/mL for the linear IV_L and 13.5 mg/mL for the cyclic IV_C. Finally, a 70 nm thickness LiF layer and a 130 nm thickness Al layer were formed by means of the thermal evaporation technique at the rate of 0.1 and 6−7 Å/s, respectively. All the fabricated EOD were stored under vacuum and in the dark until use.

The electron mobility through the active polymer layer was determined by means of a Keithley 4200 semiconductor parameter analyzer under ambient condition to provide the $J-V$ characteristics in accordance with Mott−Gurney law (eq 1)[47]

$$J = \frac{9}{8}\varepsilon_r\varepsilon_0\mu\frac{V^2}{L^3} \quad (1)$$

where the J is the current density, ε_r the relative permittivity of the material ($\approx$ 3.0), ε_0 the permittivity of a vacuum (= 8.85 × 10^{-14} F/cm), μ the charge carrier mobility, V the voltage exerted across the polymer layer, and L the thickness of active polymer layer. And the tangential line, where a slope was 2, was drawn for the log J−log V plot to estimate the μ from the intercept.[23]

Thin-Film Density Measurements. The thin film density of the linear and the cyclic polymer samples, IV_L or IV_C, was determined by the X-ray reflectometer (XRR) technique and by the combined quartz crystal microbalance (QCM)/the surface microfigure measurement. The XRR measurement was performed with X'Pert Pro MRD (Yamato Scientific Co., Ltd.) upon Cu Kα radiation (λ = 0.154 nm), equipped with a reflectivity slit and a proportional detector (PW3011/20) of a 1/8° slit, and with a 5 mm beam mask. The spin-coating solution (2.0 mg/mL for the linear IV_L and of 2.7 mg/mL for the cyclic IV_C samples) in dehydrated $CHCl_3$ was prepared for the XRR measurements, where the thinner polymer sample films in comparison with those for the EOD were employed to achieve the good fringe. The X'Pert Reflectivity 1.0 software was used to process the experimental data with the "Genetic Algorithm" as a fitting algorithm. The film density data were subsequently extracted by extrapolating the simulated fitting curve, as described before.[44]

The combined QCM/microfigure measurement provides the weight of the prescribed area and the height of thin films, respectively, and subsequently the thin film density. Thus, the solution of the linear and the cyclic polymer samples, IV_L or IV_C, in dehydrated $CHCl_3$ was spin-coated on a quartz resonator to form the thin polymer layer. The weight of the deposited polymer film was determined through the comparison of quartz resonators before and after the polymer film deposition, and the variation of frequency was expressed by the Sauerbrey equation (eq 2)[45]

$$\Delta F = -\frac{2F_0^{\,2}}{\sqrt{\rho_Q\mu_Q}}\frac{\Delta m}{A} \quad (2)$$

where ΔF is the variation of frequency, F_0 the basic frequency (9.0 MHz), Δm variation of film weight, ρ_Q the density of quartz (2.65 g/

DOI: 10.1021/acs.macromol.6b01225
Macromolecules 2016, 49, 5831−5840

cm^3), μ_Q the shearing strength of quartz (2.95×10^{11} dyn/cm^2), and A the measurement area (0.159 cm^2).

The microfigure measurement for the polymer films on the quartz resonator was then performed by using a Surfcorder ET 200 microfigure apparatus.

■ ASSOCIATED CONTENT

Supporting Information

The Supporting Information is available free of charge on the ACS Publications website at DOI: 10.1021/acs.macromol.6b01225.

Experimental section including SEC of a series of $\mathbf{I}_L$ and $\mathbf{I}_C$, and of $\mathbf{IV}_L$ before and after separation into three fractions, ^{1}H NMR spectra of linear and cyclic poly(acrylic acid)s, IR spectra of **III**/$\mathbf{TfO}^-$, **II**/**III**, and **IV**, UV−vis spectra of **III**/$\mathbf{TfO}^-$, $\mathbf{IV}_L$, and $\mathbf{IV}_C$, XRR results of a series of $\mathbf{IV}_L$ and $\mathbf{IV}_C$, and GIWAXS results of a series of $\mathbf{IV}_L$ and $\mathbf{IV}_C$ (PDF)

■ AUTHOR INFORMATION

Corresponding Author

*E-mail ytezuka@o.cc.titech.ac.jp (Y.T.).

Present Address

T.Y.: Division of Applied Chemistry, Faculty of Engineering, Hokkaido University, Sapporo, Hokkaido 060-8628, Japan.

Notes

The authors declare no competing financial interest.

■ ACKNOWLEDGMENTS

We thank the Academy for Global Leadership (A.K.). A.K. acknowledges a JSPS fellowship. The synchrotron radiation experiments were performed at BL45XU in SPring-8 with the approval of JASRI (Proposal No. 2015B1105 and 2015B1690). We thank Dr. Hiroyasu Masunaga (Japan Synchrotron Radiation Research Institute, JASRI) and Dr. Takaaki Hikima (RIKEN SPring-8 Center) for operating the GIWAXS experiments. This work was supported by KAKENHI Grant Number 26007474, and partly by KAKENHI Grant Number 26288099 (T.Y.) and 26310206 (Y.T.).

■ REFERENCES

(1) Zhang, B.; Grayson, S. M. In *Topological Polymer Chemistry: Progress of cyclic polymers in syntheses, properties and functions*; Tezuka, Y., Ed.; World Scientific: Singapore, 2013; p157.

(2) Jia, Z.; Monteiro, M. J. Synthesis of Cyclic Polymers via Ring Closure. *Adv. Polym. Sci.* **2013**, *262*, 295−328.

(3) Yamamoto, T.; Yagyu, S.; Tezuka, Y. Light- and Heat-Triggered Reversible Linear−Cyclic Topological Conversion of Telechelic Polymers with Anthryl End Groups. *J. Am. Chem. Soc.* **2016**, *138*, 3904−3911.

(4) Blencowe, A.; Qiao, G. G. Ring- Opening Metathesis Polymerization with the Second Generation Hoveyda-Grubbs Catalyst: An Efficient Approach toward High- Purity Functionalized Macrocyclic Oligo(cyclooctene)s. *J. Am. Chem. Soc.* **2013**, *135*, 5717−5725.

(5) Brown, H. A.; Waymouth, R. M. Zwitterionic Ring- Opening Polymerization for the Synthesis of High Molecular Weight Cyclic Polymers. *Acc. Chem. Res.* **2013**, *46*, 2585−2596.

(6) Kaitz, J. A.; Diesendruck, C. E.; Moore, J. S. End Group Characterization of Poly(phthalaldehyde): Surprising Discovery of a Reversible, Cationic Macrocyclization Mechanism. *J. Am. Chem. Soc.* **2013**, *135*, 12755−12761.

(7) Reisberg, S. H.; Hurley, H. J.; Mathers, R. T.; Tanski, J. M.; Getzler, Y. D. Y. L. Lactide Cyclopolymerization Kinetics, X- ray Structure, and Solution Dynamics of (tBu- SalAmEE)Al and a Cautionary Tale Of Polymetalate Formation. *Macromolecules* **2013**, *46*, 3273−3279.

(8) Kammiyada, H.; Konishi, A.; Ouchi, M.; Sawamoto, M. Ring-Expansion Living Cationic Polymerization via Reversible Activation of a Hemiacetal Ester Bond. *ACS Macro Lett.* **2013**, *2*, 531−534.

(9) Gonsales, S. A.; Kubo, T.; Flint, M. K.; Abboud, K. A.; Sumerlin, B. S.; Veige, A. S. Highly tactic cyclic polynorbornene: Stereoselective ring expansion metathesis polymerization of norbornene catalyzed by a new tethered tungsten-alkylidene catalyst. *J. Am. Chem. Soc.* **2016**, *138*, 4996−4999.

(10) *Topological Polymer Chemistry: Progress of cyclic polymers in syntheses, properties and functions*; Tezuka, Y., Ed.; World Scientific: Singapore, 2013.

(11) Yamamoto, T.; Tezuka, Y. Cyclic polymers revealing topology effects upon self-assemblies, dynamics and responses. *Soft Matter* **2015**, *11*, 7458−7468.

(12) Grayson, S. M., Getzler, Y. D. Y. L., Zhang, D., Eds.; *Cyclic polymers: New developments, Special issue in Reactive and Functional Polymers*, 2014; Vol. *80*.

(13) Zhang, K.; Lackey, M. A.; Wu, Y.; Tew, G. N. Universal cyclic polymer templates. *J. Am. Chem. Soc.* **2011**, *133*, 6906−6909.

(14) Zhang, K.; Zha, Y.; Chen, Y.; Tew, G. N. Metallo-supramolecular cyclic polymers. *J. Am. Chem. Soc.* **2013**, *135*, 15994−15997.

(15) Schappacher, M.; Deffieux, A. Synthesis of macrocyclic copolymer brushes and their self-assembly into supramolecular tubes. *Science* **2008**, *319*, 1512−1515.

(16) Doi, Y.; Iwasa, Y.; Watanabe, K.; Nakamura, M.; Takano, A.; Takahashi, Y.; Matsushita, Y. Synthesis and characterization of comb-shaped ring polystyrenes. *Macromolecules* **2016**, *49*, 3109−3115.

(17) Zhang, S.; Yin, L.; Zhang, W.; Zhang, Z.; Zhu, X. Synthesis of diverse cyclic-brush polymers with cyclic polystyrene as a universal template via a grafting-from approach. *Polym. Chem.* **2016**, *7*, 2112−2120.

(18) Williams, R. J.; Pitto-Barry, A.; Kirby, N.; Dove, A. P.; O'Reilly, R. K. Cyclic graft copolymer unimolecular micelles: effects of cyclization on particle morphology and thermoresponsive behavior. *Macromolecules* **2016**, *49*, 2802−2813.

(19) Würthner, F.; Saha-Möller, C. R.; Fimmel, B.; Ogi, S.; Leowanawat, P.; Schmidt, D. Perylene bisimide dye assemblies as archetype functional supramolecular materials. *Chem. Rev.* **2016**, *116*, 962−1052.

(20) Foster, S.; Finlayson, C. E.; Keivanidis, P. E.; Huang, Y.-S.; Hwang, I.; Friend, R. H.; Otten, M. B. J.; Lu, L.-P.; Schwartz, E.; Nolte, R. J. M.; Rowan, A. E. *Macromolecules* **2009**, *42*, 2023−2030.

(21) Spreitler, F.; Sommer, M.; Hollfelder, M.; Thelakkat, M.; Gekle, S.; Köhler, J. Unravelling the conformations of di-(perylene bisimide acrylate) by combining time-resolved fluorescence-anisotropy experiments and molecular modelling. *Phys. Chem. Chem. Phys.* **2014**, *16*, 25959−25968.

(22) Lohwasser, R. H.; Gupta, G.; Kohn, P.; Sommer, M.; Lang, A. S.; Thurn-Albrecht, T.; Thelakkat, M. Phase separation in the melt and confined crystallization as the key to well-ordered microphase separated donor-acceptor block copolymers. *Macromolecules* **2013**, *46*, 4403−4410.

(23) Gupta, G.; Singh, C. R.; Lohwasser, R. H.; Himmerlich, M.; Krischok, S.; Müller-Buschbaum, P.; Thelakkat, M.; Hoppe, H.; Thurn-Albrecht, T. Morphology, crystal structure and charge transport in donor acceptor block copolymer thin films. *ACS Appl. Mater. Interfaces* **2015**, *7*, 12309−12318.

(24) Chi, C.-Y.; Chen, M.-C.; Liaw, D.-J.; Wu, H.-Y.; Huang, Y.-C.; Tai, Y. A bifunctional copolymer additive to utilize photoenergy transfer and to improve hole mobility for organic ternary bulk-heterojunction solar cell. *ACS Appl. Mater. Interfaces* **2014**, *6*, 12119−12125.

(25) Ullah, M.; Tandy, K.; Li, J.; Shi, Z.; Burn, P. L.; Meredith, P. High-mobility, heterostructure light-emitting transistors and complementary inverters. *ACS Photonics* **2014**, *1*, 954−959.

DOI: 10.1021/acs.macromol.6b01225
Macromolecules 2016, 49, 5831−5840

(26) Kohn, P.; Ghazaryan, L.; Gupta, G.; Sommer, M.; Wicklein, A.; Thelakkat, M.; Thurn-Albrecht, T. Thermotropic behavior, packing, and thin film structure of an electron accepting side-chain polymer. *Macromolecules* **2012**, *45*, 5676−5683.
(27) Dou, X.; Sabba, D.; Mathews, N.; Wong, L. H.; Lam, Y. M.; Mhaisalkar, S. Hydrothermal synthesis of high electron mobility Zn-doped SnO_2 nanoflowers as photoanode material for efficient dye-sensitized solar cells. *Chem. Mater.* **2011**, *23*, 3938−3945.
(28) Hufnagel, M.; Muth, M.-A.; Brendel, J. C.; Thelakkat, M. Fullerene-grafted copolymers exhibiting high electron mobility without nanocrystal formation. *Macromolecules* **2014**, *47*, 2324−2332.
(29) Oike, H.; Imaizumi, H.; Mouri, T.; Yoshioka, Y.; Uchibori, A.; Tezuka, Y. Designing unusual polymer topologies by electrostatic self-assembly and covalent fixation. *J. Am. Chem. Soc.* **2000**, *122*, 9592−9599.
(30) Li, D.; Dong, G.; Duan, L.; Wang, L.; Qiu, Y. New method of mobility measurement for organic semiconductors by optoelectronic coupling. *J. Phys. Chem. C* **2012**, *116*, 5235−5239.
(31) Oike, H.; Imamura, H.; Tezuka, Y. Synthesis of poly(tetrahydrofuran) polymacromonomers having mixed branch segments through reshuffling in electrostatic self-assembly and subsequent covalent fixation. *Macromolecules* **1999**, *32*, 8816−8820.
(32) Oike, H.; Imamura, H.; Tezuka, Y. Control in both backbone and branch segment length of poly(tetrahydrofuran) polymacromonomers by electrostatic self-assembly and covalent fixation. *Macromolecules* **1999**, *32*, 8666−8670.
(33) Foston, M.; Hubbell, C.; Park, D.-H.; Cook, F.; Tezuka, Y.; Beckham, H. W. Surface modification by electrostatic self-assembly followed by covalent fixation. *Angew. Chem., Int. Ed.* **2012**, *51*, 1849−1852.
(34) Matyjaszewski, K.; Xia, J. Atom transfer radical polymerization. *Chem. Rev.* **2001**, *101*, 2921−2990.
(35) Baba, E.; Yatsunami, T.; Yamamoto, T.; Tezuka, Y. A study on emulsion stabilization induced with linear and cyclized polystyrene-poly(ethylene oxide) block copolymer surfactants. *Polym. J.* **2015**, *47*, 408−412. In the applied condition, the polydispersity of the linear precursors tends to be broadened, as the end-capping reaction does not proceed instantaneously.
(36) Mohamad, D. K.; Fischereder, A.; Yi, H.; Cadby, A. J.; Lidzey, D. G.; Iraqi, A. A novel 2,7-linked carbazole based "double cable" polymer with pendant perylene diimide functional groups: preparation, spectroscopy and photovoltaic properties. *J. Mater. Chem.* **2011**, *21*, 851−862.
(37) Suzuki, T.; Yamamoto, T.; Tezuka, Y. Constructing a macromolecular $K_{3,3}$ graph through electrostatic self-assembly and covalent fixation with a dendritic polymer precursor. *J. Am. Chem. Soc.* **2014**, *136*, 10148−10155.
(38) Appel, W. P. J.; Nieuwenhuizen, M. M. L.; Meijer, E. W. Multiple Hydrogn-Bonded Supramolecular Polymers. In *Supramolecular Polymer Chemistry*; Harada, A., Ed.; Wiley-VCH: Weinheim, 2012; pp 3−28.
(39) SEC separation of the product, $\mathbf{IV}_L$ and $\mathbf{IV}_C$, into three fractions and the repeated SEC measurements for each fraction were carried out (Figure S4) to show the profile similar to that before fractionation.
(40) De Witte, P. A. J.; Hernando, J.; Neuteboom, E. E.; van Dijk, E. M. H. P.; Meskers, S. C. J.; Janssen, R. A. J.; van Hulst, N. F.; Nolte, R. J. M.; García-Parajó, M. F.; Rowan, A. E. Synthesis and characterization of long perylenediimide polymer fibers: from bulk to the single-molecule level. *J. Phys. Chem. B* **2006**, *110*, 7803−7812.
(41) Steyrleuthner, R.; Bange, S.; Neher, D. Reliable electron-only devices and electron transport in *n*-type polymers. *J. Appl. Phys.* **2009**, *105*, 064509.
(42) Blom, P. W. M.; de Jong, M. J. M.; Vleggaar, J. J. M. Electron and hole transport in poly(*p*-phenylene vinylene) devices. *Appl. Phys. Lett.* **1996**, *68*, 3308−3310.
(43) Verilhac, J.-M.; Pokrop, R.; LeBlevennec, G.; Kulszewicz-Bajer, I.; Buga, K.; Zagorska, M.; Sadki, S.; Pron, A. Molecular weight dependent charge carrier mobility in poly(3,3″-dioctyl-2,2′:5′,2″-terthiophene). *J. Phys. Chem. B* **2006**, *110*, 13305−13309.
(44) Fladischer, S.; Neuhold, A.; Kraker, E.; Haber, T.; Lamprecht, B.; Salzmann, I.; Resel, R.; Grogger, W. Diffusion of Ag into organic semiconducting materials: a combined analytical study using transmission electron microscopy and X-ray reflectivity. *ACS Appl. Mater. Interfaces* **2012**, *4*, 5608−5612.
(45) Sauerbrey, G. *Eur. Phys. J. A* **1959**, *155*, 206−222.
(46) Oike, H.; Kobayashi, S.; Tezuka, Y.; Goethals, E. J. Bis(triflate ester)s having an additional functional group: initiators for preparation of α,ω,kentro-telechelic poly(THF)s. *Macromolecules* **2000**, *33*, 8898−8903.
(47) Mott, N. F.; Gurney, R. W. *Electronic Processes in Ionic Crystals*; The Clarendon Press: Oxford, UK, 1940.

DOI: 10.1021/acs.macromol.6b01225
Macromolecules 2016, 49, 5831−5840